

Synthesis of cellulose–nanohydroxyapatite composite in 1-*n*-butyl-3-methylimidazolium chloride

S. Zadegan^a, M. Hossainipour^a, H. Ghassai^a, H.R. Rezaie^{a,*}, M.R. Naimi-Jamal^b

^aDepartment of Metallurgy & Materials Engineering, Iran University of Science & Technology, Narmak, Tehran 16844, Iran

^bDepartment of Chemistry, Iran University of Science & Technology, Iran

Received 24 March 2010; received in revised form 8 April 2010; accepted 14 June 2010

Available online 3 August 2010

Abstract

In this study cellulose–nanohydroxyapatite composite was fabricated for bone tissue engineering applications. In this composite a natural biopolymer was reinforced with bioactive nanohydroxyapatite for replacement or healing of bone. The ionic liquid 1-*n*-butyl-3-methylimidazolium chloride (BmimCl) was used for dissolution of cellulose.

Nanohydroxyapatite (n-HAp) powder was characterized by X-ray diffractometry (XRD), scanning electron microscopy (SEM) and FT-infrared (FTIR) spectroscopy. Thermogravimetric analysis (TGA) as well as MTT assay of nanocomposite was conducted to assess the thermal stability and cytotoxicity of the samples.

The results of XRD showed the formation of hydroxyapatite crystals and also SEM images indicated that n-HAp powder was nanocrystalline. The composite was thermally less stable than native cellulose. Also native cellulose had higher decomposition rate and mass loss. Results of biological test showed that the samples were biocompatible with no toxicity. Also, SEM observations demonstrated that human osteoblast cells can attach to the surface of the nanocomposite samples and this composite can be used as bone tissue engineering.

© 2010 Elsevier Ltd and Techna Group S.r.l. All rights reserved.

Keywords: Cellulose; Nanohydroxyapatite; Ionic liquid

1. Introduction

A variety of materials have been used for replacement and repair of damaged or traumatized bone tissues [1–3]. These materials include metals, ceramics, polymers (natural and synthetic) and their combinations. Metals and ceramics have two major disadvantages for tissue engineering applications: they are lack of degradability in a biological environment, and their processability is very limited [4]. In contrast, polymers have great design flexibility because the composition and structure can be tailored to specific needs. They are therefore attractive candidate. Biodegradability can be imparted into polymers through molecular design [5]. However, polymers have lower modulus and strength as compared to metals and ceramics [6]. For the mechanical reinforcement of polymers or for certain applications such as bone regeneration, composite materials of biopolymers and bioceramics have been produced

for bone tissue engineering [7]. The most frequently used bioceramic material is hydroxyapatite (HAp). It is bioactive, osteoconductive, non-toxic and non-immunogenic [8]. Many efforts have been made to modify HA by polymers since the natural bone is a composite mainly consisted of nano-sized, needle-like HAp crystals (accounts for about 65 wt% of bone) and collagen fibers [9,10].

Natural biodegradable polymers have been used in tissue engineering [11,12]. One important category of natural biopolymers is polysaccharides. Cellulose is an abundant renewable polysaccharide consisting of a linear chain of (1,4) linked β -D-glucopyranose units aggregated to form a highly ordered structure due to its chemical constitution and spatial conformation [13] (Fig. 1).

The individual cellulose chains are joined by a network of inter- and intra-molecular hydrogen bonding and van der Waals forces. The crystalline structure of cellulose, due to hydrogen bonds, in combination with the high molecular weight, gives it unique properties like chemical stability and mechanical strength. In the biomedical field, cellulose and its derivatives have been extensively used for decades [14].

* Corresponding author.

E-mail address: hrezaie@iust.ac.ir (H.R. Rezaie).

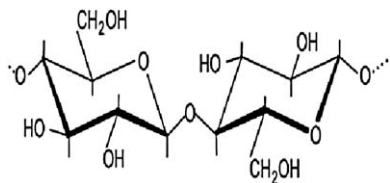


Fig. 1. The cellulose molecule – $(C_6H_{10}O_5)_n$ – in its chair configuration [13].

The biocompatibility of several celluloses is well established. Cellulose has a long background in medical applications, essentially due to its lack of toxicity, water solubility or high swelling ability and stability to temperature and pH variations [15].

However, processing and derivatization of cellulose are difficult in general, because this natural polymer is neither meltable nor soluble in conventional solvents due to its hydrogen bonded and partially crystalline structure. Over the past decades, several solvent systems have been developed for manufacturing cellulose materials. Typical examples for these solvents include LiCl/N,N-dimethylacetamide (DMAc), LiCl/N-methyl-2-pyrrolidone (NMP), dimethyl sulfoxide (DMSO)/paraformaldehyde, and N-methyl morpholine-N-oxide (NMMO) [16,17]. However, the above solvent systems are limited to their dissolving capability, toxicity, high cost, solvents recovery, uncontrollable side reaction, and instability during cellulose processing and/or derivatization [16].

Recently, ionic liquids (ILs) were found to dissolve native cellulose. ILs are organic salts with polar character and low melting points ($<100^\circ\text{C}$) [18]. They are thermally and chemically stable and have a practically non-detectable vapor pressure. Their non-volatile nature allows for easy recycling after usage and, thus, places them high in the realm of green chemistry [19]. Quite few ionic liquids are known and have been used to dissolve cellulose. The most frequently used are the hydrophilic ILs 1-*n*-butyl-3-methylimidazolium chloride (BmimCl) and 1-allyl-3-methylimidazolium chloride (AmimCl).

The dissolution mechanism of cellulose in ionic liquids involves the oxygen and hydrogen atoms of cellulose-OH in the formation of electron donor–electron acceptor complexes which interact with the ionic liquid (Fig. 2).

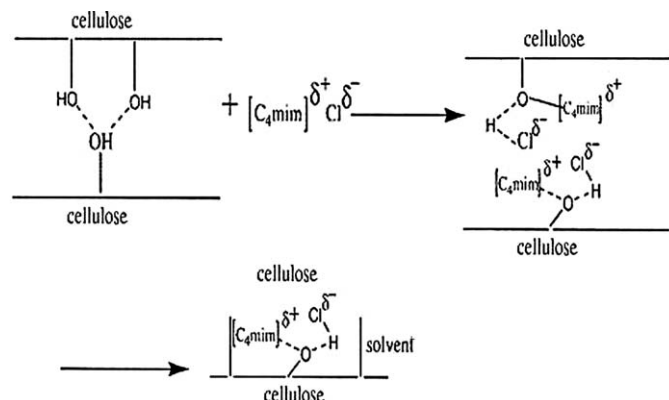


Fig. 2. Dissolution of cellulose in ionic liquids [19].

For their interaction, the cellulose atoms serve as electron pair donor and hydrogen atoms act as an electron acceptor [19].

In the present study, cellulose and cellulose–hydroxyapatite composites were successfully prepared and then were characterized.

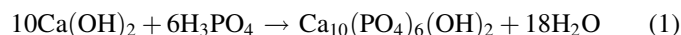
2. Experimental

2.1. Materials and methods

Microcrystalline cellulose (MCC), calcium hydroxide $(Ca(OH)_2)$ and orthophosphoric acid (H_3PO_4) were purchased from Merck and 1-*n*-butyl-3-methylimidazolium chloride (BmimCl) and other chemical materials were received from Sigma–Aldrich.

2.2. Preparation of nanoHAp (n-HAp)

n-HAp with Ca/P ratios of 1.67 was synthesized by a wet chemical precipitation reaction between $Ca(OH)_2$ and H_3PO_4 [20]. 0.5 M $Ca(OH)_2$ powder was added slowly into deionized water at 25°C and vigorously agitated for 1 h. To this solution a 0.3 M H_3PO_4 solution was added dropwise with ratio of 6 ml/min approximately to produce a white precipitate. The pH was controlled to a minimum of 8.0 ± 1.0 during the addition of acid to the $Ca(OH)_2$ suspension using a 1.0 M NH_4OH solution. The solution rested at room temperature for 24 h. After decantation, the precipitates were washed for three consecutive times with deionized water and dried at 75°C for 12 h. Then, the powders were milled and passed through sieve set of 200 mesh.



For characterizing the crystal phases of n-HAp, XRD (JDX-8030 JEOL, Cu $K\alpha$) and FTIR (SHIMADZU, 8400S) were performed on the powder. The morphology of particles was analyzed on SEM (Philips, XL300). From the full width at half maximum (FWHM), the average crystalline size calculated with the (0 0 2) diffraction peaks in the peak in the XRD pattern according to the Scherrer formula:

$$d = \frac{0.9\lambda}{\beta \cos \alpha} \quad (2)$$

where d is the crystallite size (nm), λ is the wavelength of the X-ray ($\lambda_{Cu} = 0.154056$ nm), α is the peak diffraction angle ($^\circ$) and β is the experimental full width at half maximum [21].

2.3. Preparation of cellulose solution in BmimCl

The solution of cellulose in BmimCl (3%, w/w) was obtained by continuous stirring of the starting materials at 95°C for 5 h. After complete dissolution of cellulose, an appropriate mass of nanohydroxyapatite (n-HAp) particles were added in order to obtain composites with n-HAp load of 0.16 (16% n-HAp and 84% cellulose, w/w) and stirred for 15 min. Sonication was then applied four times for 5 min each, a total of 20 min. After preparation, the solution was poured in a

petri dish and allowed to stand for 30 min at 4 °C and then immersed in water and kept at 4 °C.

For preparation of regenerated cellulose film the solution was cast onto a glass plate to give a thickness of about 0.5 mm, took off air bubble in a vacuum oven, and then immediately coagulated in water to obtain a transparent regenerated cellulose gel. The regenerated cellulose gel was washed with distilled water and then dried at 60 °C in a vacuum oven. The recovery of ILs was accomplished by evaporating water from the precipitation liquids.

Composite samples were examined by XRD and TGA (Shimadzu, model TGA-50) with a heating rate of 10 °C/min until 80 °C in air, hold for 5 min, and then with a heating rate of 10 °C/min until 600 °C. The mass at 150 °C was set as 100% mass. The regenerated cellulose was examined by FTIR spectra.

2.4. In vitro cell test

2.4.1. Cell culture

The human osteoblast cells were cultured in Dulbecco's modified medium F-12 nutrient mixture (DMEM/F12, Invitrogen GmbH, Karlsruhe, Germany) supplemented with 10% fetal calf serum (FCS, Invitrogen GmbH, Karlsruhe, Germany) and 1% penicillin/streptomycin (Invitrogen GmbH, Karlsruhe, Germany). Cells were plated into cell culture flasks and incubated at 37 °C and 5% CO₂. Medium was changed every 3 days.

2.4.2. Cell proliferation

The proliferation rate of osteoblast cells next to the composite samples was measured using dimethylthiazol diphenyl tetrazolium bromide (MTT) assay. Briefly, all the cell-loaded composites were placed in a 24 well flat-bottom culture plate after cultured for 3, 7 and 14 days, and 100 µl of MTT solution (5 mg/ml in PBS) added to each sample after the samples were incubated at 37 °C for 4 h to allow MTT formazan formation, the upper solvent was removed and 100 µl of acidic isopropanol (0.04 M HCl in isopropanol) was added to each well to dissolve the formazan crystals for 4 h at 37 °C and the optical density (OD) at 570 nm was determined by Elisa Reader (EPSON, LQ-300) [22]. The wells without composite samples were used as negative controls.

2.4.3. SEM examination of cell-seeded composites

After being cultured for 3 days, the specimens with attached cells were rinsed twice with PBS (Ph 7.4), and immersed in PBS containing 2% glutaraldehyde for 4 h to fix the cells, followed by rinsing twice with PBS for 10 min. They were dehydrated through a graded series of ethanol solutions (30%, 50%, 70%, 90%, 95%) for 10 min each and with 100% ethanol for additional 30 min, being allowed to air-dry at least 10 h. The dry cell-seed composites were mounted on aluminum stubs, sputter-coated in vacuum with gold–palladium and examined by a scanning electron microscope.

2.4.4. Statistical analysis

All data are presented as means ± standard deviation (SD) for $n = 3$. Statistical comparisons were performed using

Students's *t*-test. *P*-values <0.05 were considered statistically significant.

3. Results and discussion

3.1. Characterization of n-HAp particles

Around 60% of bone is made of HAp on the nanometer scale and therefore it is evident why HAp has intensively investigated as the major component of composite materials for bone tissue engineering. Recent research suggested that if synthetic HAp could resemble bone minerals more in composition, size and morphology better osteoconductivity would be achieved [23,24]. Webster et al. have shown significant increase in protein absorption and osteoblast adhesion on the nano-sized ceramic materials compared to traditional micron-sized ceramic materials [25,26].

The XRD pattern of the n-HAp powder indicated the presence of all major HAp peaks, such as (0 0 2), (2 1 1) and (3 0 0) at 25.8, 31.7 and 32.9 which are shown in Fig. 3. The results revealed that the powders were crystalline and no second phases such as tricalcium phosphate (TCP) and calcium oxide were detected. The average crystalline size $d_{(0\ 0\ 2)}$ determined from X-ray broadening analysis was about 15 nm.

Fig. 4 shows the FTIR spectrum of n-HAp, the two bands at 560–600 and 1030–1090 cm⁻¹ ranges are due to stretching vibration of phosphate groups. The OH⁻¹ bands were observed at 630 and 3740 cm⁻¹, and the peak in 1400–1600 cm⁻¹ range indicated the existence of CO₃²⁻ group in the structure. From these measurements, the precipitate particles are proved to be n-HAp.

The XRD pattern and FTIR spectrum of synthesized HAp was confirmed with pioneer articles [27–30].

SEM image of the n-HAp powders is shown in Fig. 5. It shows that the sizes of the particles are in the range of 50–100 nm. Also,

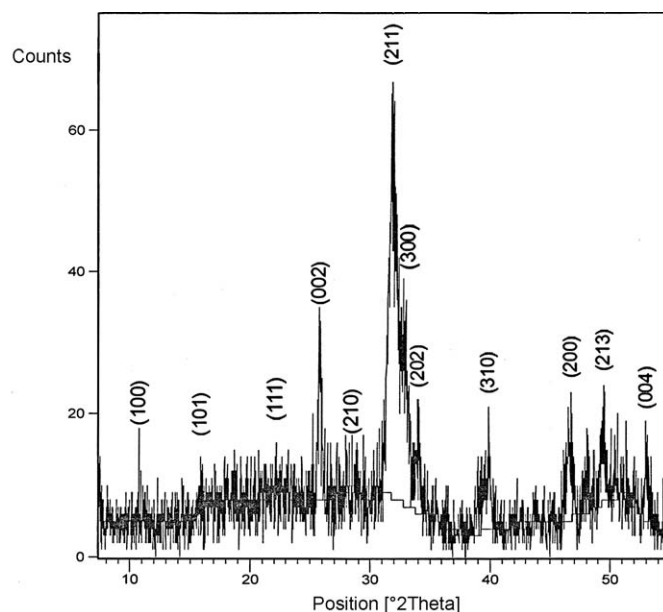


Fig. 3. X-ray diffraction pattern of n-HAp.

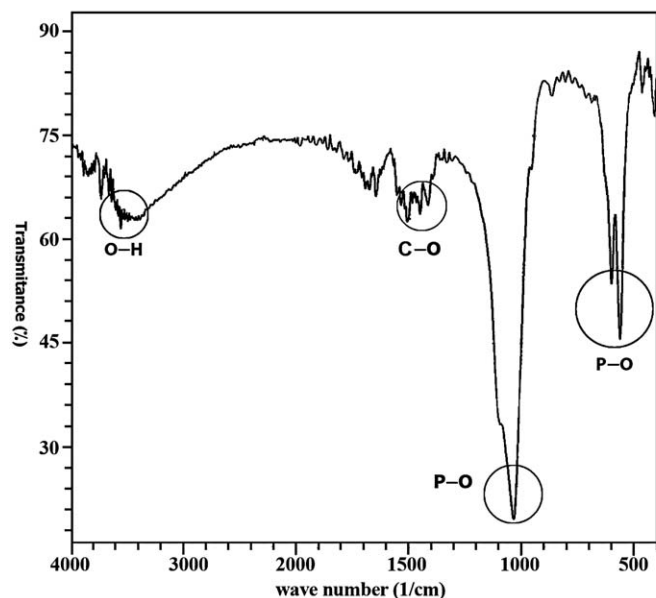


Fig. 4. FTIR spectrum of n-HAp.

several primary nanoparticles form the cabbage shape agglomerates with submicron size.

3.2. Characterization of regenerated cellulose film from *BmimCl*

It is generally recognized that, in order to dissolve cellulose, to disrupt its great number of inter- and intra-molecular hydrogen bonds is required. In the case of ionic liquid *BmimCl* used as solvent for cellulose, the relatively high chloride concentration and activity in this IL were thought to play the key role in dissolving cellulose [31]. Therefore, for investigation chemical reactions during dissolution of cellulose in *BmimCl*, the FTIR spectra of cellulose before and after regeneration were recorded. In Fig. 6, it can be seen that the two spectra are quite similar, and no new peaks appear in the regenerated samples, indicating no chemical reaction occurred

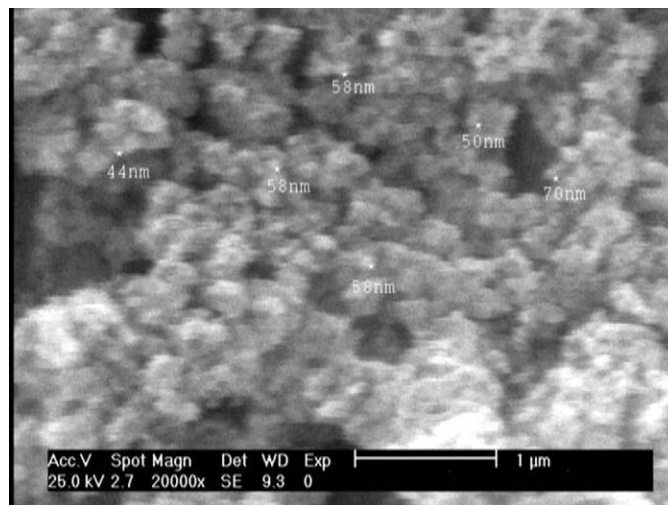


Fig. 5. SEM image of n-HAp particles.

during the dissolution and coagulation processes of the cellulose. In other words, *BmimCl* was a direct solvent for cellulose.

3.3. Characterization of composite from *BmimCl*

Although native cellulose is thermally the most stable from the cellulose composite, it had the highest mass loss in thermogravimetric analysis. Similar results have been reported in the literature for other types of cellulose regenerated from *BmimCl* [31]. The decomposition rates for regenerated cellulose and 0.16 HAp composites are the same but are different from native cellulose. The representative data from the thermogravimetric analysis are summarized in Table 1.

Mechanical properties of the polymer/ceramic composites used for bone tissue engineering are strongly dependent on the nanometer size of the inorganic component and uniform distribution of it in the polymer matrix; hence, mixing will be a critical unit operation in this regard [32]. Because of high

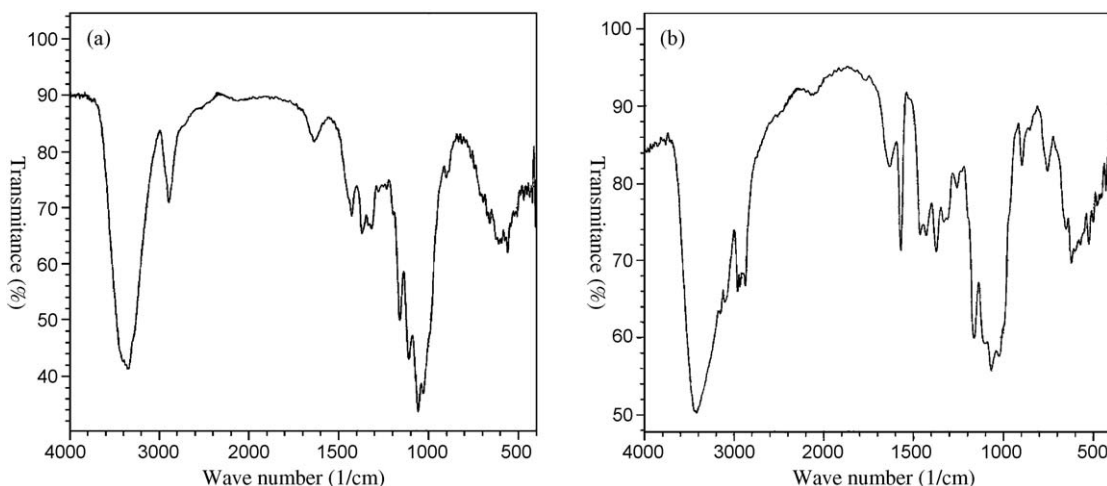


Fig. 6. FTIR spectra of (a) original cellulose and (b) regenerated cellulose.

Table 1
Results from thermogravimetric analysis.

Material	Temperature of 98% remaining mass (°C)	Temperature of maximum decomposition rate (°C)
Native cellulose	275	345
Cellulose–0.16 HAp	260	315
Regenerated cellulose	235	315

viscosity of cellulose solvent in BmimCl and tendency of n-HAp to agglomeration it was important to study the dispersion of n-HAp in cellulose matrix.

The surface of nanocomposite samples was investigated using scanning electron microscope. The P-map image showed that the distribution of phosphor in the matrix was almost homogeneous and the time of sonication was enough for n-HAp dispersion in cellulose solvent (Fig. 7).

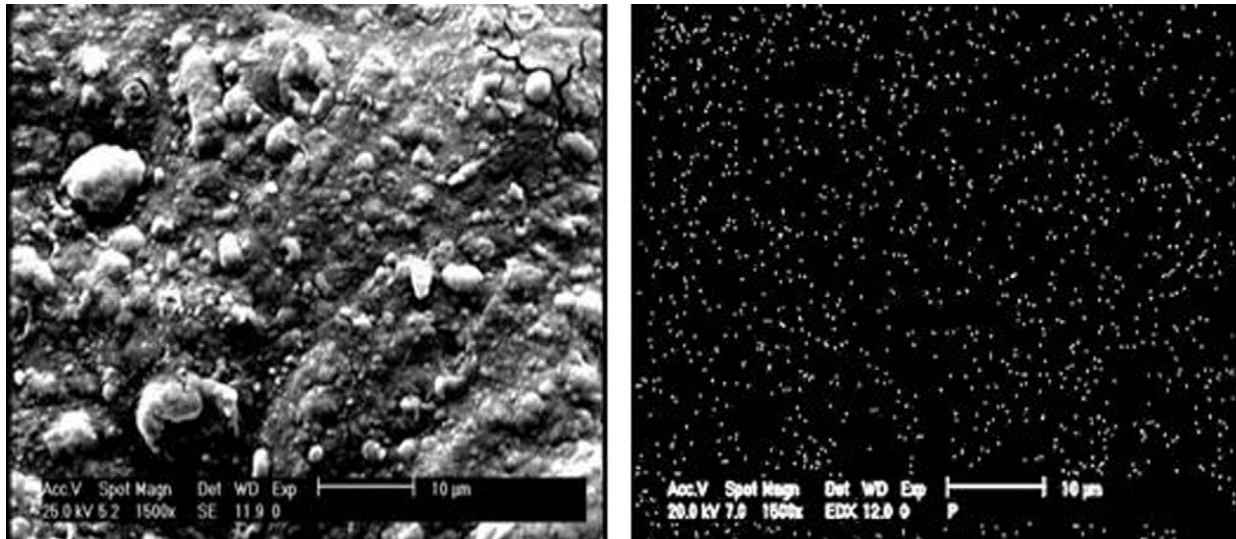


Fig. 7. P-map of cellulose–16% n-HAp composite.

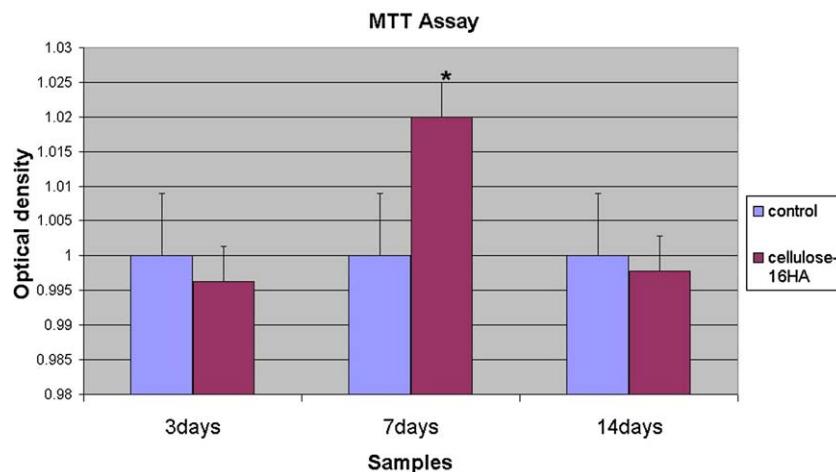


Fig. 8. MTT assay of osteoblast cells were cultured on composite.

3.4. Biocompatibility examination

Investigation on the proliferation of osteoblast cells is an important technique to evaluate the biocompatibility of biomaterials in vitro [33]. This assay measures the metabolic activity of the cells, which can be correlated with the number of viable cells. In this study the proliferation on n-HAp/cellulose composite was evaluated by MTT assay.

The results by MTT assay were compared with control group as shown in Fig. 8. From the data in Fig. 8, the cell numbers were increased with the culture time on composites and the viability of cultured cells on the composites were near the control and there was a significant difference in biocompatibility between control and nanocomposite groups ($P > 0.05$) at day 7. The results of biological test showed that the samples were biocompatible until 14 days and had no toxicity. Also n-HAp composite samples promoted proliferation and growth of the cells, which indicated their bioactivity properties.

A rapid and strong adhesion of osteoblast on composite successfully is therefore an essential factor for successful bone

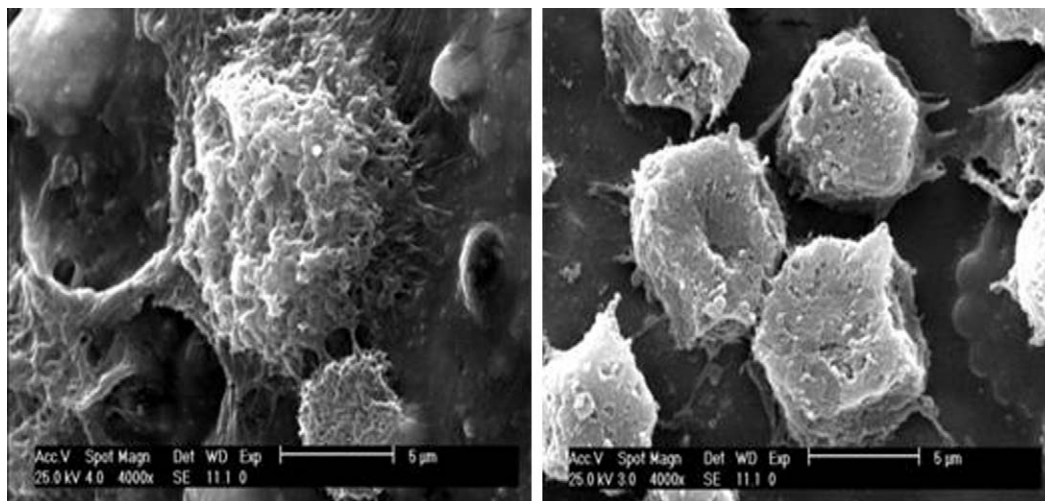


Fig. 9. SEM images of human osteoblast cells were cultured on composite.

growth [34]. n-HAp was used in composite to increase surface area and improve cell adhesion and proliferation.

Fig. 9 shows SEM micrographs of osteoblast cells on the composite surface after 3 days of culture. It can be seen that the cells had been able to attach on the surface of composite and appeared to show normal morphology with cell size 5 µm in diameter. By electronic microscope diagrams it can be shown that the reproduced cells on composite surfaces enjoy a natural figure with cytoplasmic wastes contacting directly and appropriate communications with adjacent cells.

4. Conclusion

The present study employed a wet chemical precipitation method for the production of n-HAp at low temperature with easy fabrication technique and showed that cellulose–nanohydroxyapatite can be a good candidate for bone tissue engineering. Thus, BmimCl solution and other ionic liquids open new possibilities for the otherwise difficult treatment of biomacromolecules. The properties of these new materials make them promising especially for bone regeneration applications.

References

- [1] L.L. Hench, J.M. Polak, Third-generation biomedical materials, *J. Sci.* 245 (2002) 1014–1017.
- [2] R. Langer, Biomaterials: status, challenges, and perspectives, *J. AIChE* 46 (2000) 1286–1289.
- [3] T. Livingston, P. Ducheyne, J. Garino, In vivo evaluation of a bioactive scaffold for bone tissue engineering, *J. Biomed. Mater. Res.* 62 (2002) 1–13.
- [4] V. Maquet, R. Jerome, Design of macroporous biodegradable polymer scaffolds for cell transplantation, *J. Mater. Sci. Forum.* 250 (1997) 15–42.
- [5] J.C. Middleton, A.J. Tipton, Synthetic biodegradable polymers as orthopedic devices, *J. Biomater.* 21 (2000) 2335–2346.
- [6] S. Ramakrishna, J. Mayer, K. Leong, Biomedical applications of polymer–composite materials: a review, *J. Compos. Sci. Technol.* 61 (2001) 1189–1224.
- [7] J. Jordan, K. Jacob, R. Tannenbaum, Experimental trends in polymer nanocomposites: a review, *J. Mater. Sci. Eng.* 393 (2005) 1–11.
- [8] R. Murugan, S. Ramakrishna, Development of nanocomposites for bone grafting, *J. Compos. Sci. Technol.* 65 (2005) 2385–2406.
- [9] F. Wang, M. Li, Y. Lu, Y. Qi, Y. Liu, Synthesis and microstructure of hydroxyapatite nanofibers synthesized at 37 °C, *J. Mater. Chem. Phys.* 95 (2006) 145–149.
- [10] S. Koutsopoulos, Synthesis and characterization of hydroxyapatite crystals: a review study on the analytical methods, *J. Biomed. Res.* 62 (2002) 600–612.
- [11] C. Tsiptsias, L. Tsivintzelis, L. Papadopoulou, C. Panayiotou, A novel method for producing tissue engineering scaffolds from chitin, chitin–hydroxyapatite, and cellulose, *J. Mater. Sci. Eng. C* (2008) 1–6.
- [12] I. Simkovic, What could be greener than composites made from polysaccharides? *J. Carbohydr. Polym.* 74 (2008) 759–762.
- [13] R. Swatoski, S. Spear, J. Holbrey, R. Rogers, Dissolution of cellulose with ionic liquids, *J. Am. Chem. Soc.* 124 (18) (2002) 4974–4979.
- [14] D. Chauveaux, C. Barbie, X. Barthe, C. Baquey, Biological behaviour of cellulosic materials after bone implantation: preliminary results, *J. Clin. Mater.* 5 (1990) 251–258.
- [15] N. Hoenich, Cellulose for medical applications: past, present and future, *J. Bioresour.* 1 (2) (2006) 270–280.
- [16] H. Zhang, J. Wu, J. Zhang, J. He, 1-Allyl-3-methylimidazolium chloride room temperature ionic liquids: a new and powerful nonderivatizing solvent for cellulose, *J. Macromol.* 38 (2004) 8272–8277.
- [17] Ca. Yan, W. Jun, L. Huiquan, Y. Zhang, H. Jiasong, Room temperature ionic liquids (RTILs): a new and versatile platform for cellulose processing and derivatization, *J. Chem. Eng.* 147 (2009) 13–21.
- [18] T. Heinze, K. Schwikal, S. Barthel, Ionic, liquids as reaction medium in cellulose functionalization, *J. Macromol. Biol. Sci.* 5 (2005) 520–525.
- [19] L. Feng, Z. Chen, Research progress on dissolution and functional modification of cellulose in ionic liquids, *J. Mol. Liq.* 142 (2008) 1–5.
- [20] C. Kothapalli, M. Wei, A. Vasiliev, Influence of temperature and concentration on the sintering behaviour and mechanical properties of hydroxyapatite, *J. Acta Mater.* 52 (2004) 5655–5663.
- [21] G. Koumoulidis, A. Katsoulidis, C. Pomonis, T. Sdoulos, Preparation of hydroxyapatite via microemulsion route, *J. Colloid Interface Sci.* 259 (2003) 254–260.
- [22] G. Zund, Q. Ye, S.P. Hoerstrup, A. Scheoberlein, J. Grunfelder, Tissue engineering in cardiovascular surgery: MTT, a rapid and reliable quantitative method to assess the optimal human cell seeding on polymeric meshes, *Eur. J. Cardiothorac. Surg.* 5 (4) (1999) 519–524.
- [23] C. Du, F. Cui, X. Zhu, K. Groot, Three-dimensional nano-HAp/collagen matrix loading with osteogenic cells in organ culture, *J. Biomed. Mater. Res.* 44 (1999) 407–415.
- [24] C. Du, F. Cui, Ql. Feng, X. Zhu, K. Groot, Tissue response to nano-hydroxyapatite/collagen composite implants in marrow cavity, *J. Biomed. Mater. Res.* 42 (1998) 540–548.

- [25] Tj. Webster, C. Ergun, Rh. Doremus, R.W. Siegel, R. Bizios, Specific proteins mediate enhanced osteoblast adhesion on nanophase ceramics, *J. Biomed. Mater. Res.* 51 (2000) 475–483.
- [26] Tj. Webster, C. Ergun, Rh. Doremus, R.W. Siegel, R. Bizios, Osteoblast adhesion on nanophase ceramics, *J. Biomater.* 20 (1999) 1221–1227.
- [27] J. Huang, Y. Lin, X. Fu, S. Best, Development of nano-sized hydroxyapatite reinforced composites for tissue engineering scaffolds, *J. Mater. Med.* 18 (2007) 2151–2157.
- [28] Y. Ota, T. Iwashita, T. Kasuga, Novel preparation method of hydroxyapatite fibers, *J. Am. Ceram. Soc.* 81 (1998) 1665–1668.
- [29] C. Kothapalli, M. Wei, A. Vasiliev, M. Shaw, Influence of temperature and concentration on the sintering behaviour and mechanical properties of hydroxyapatite, *J. Acta Mater.* 52 (2004) 5655–5663.
- [30] D. Choia, K. Marra, P. Kumta, Chemical synthesis of hydroxyapatite/poly(ϵ -caprolactone) composites, *J. Mater. Res. Bull.* 39 (2004) 417–432.
- [31] R. Swatloski, S. Spear, J. Holbrey, R. Rogers, Dissolution of cellulose with ionic liquids, *J. Am. Chem. Soc.* 124 (2002) 4974–4975.
- [32] F. Lange, L. Miller, L. Hofmann, P. Greil, M. Wenzel, A colloidal method to ensure phase homogeneity in β -Al₂O₃/ZrO₂ composite systems, *J. Am. Ceram. Soc.* 70 (2005) 896–900.
- [33] X. Cheng, Y. Li, Y. Zuo, L. Zhang, H. Wang, Properties and in vitro biological evaluation on nano-hydroxyapatite/chitosan membranes for bone guided regeneration, *J. Mater. Sci. Eng.* 29 (2009) 29–35.
- [34] Oh. Seunghan, D. Chiara, R. Thomas, R. Rita, Significantly accelerated osteoblast cell growth on aligned TiO₂ nanotubes, *J. Inter. Sci.* 70 (2005) 96–103.